

Collision-Free Stable Polygon Formation of Multi-Agent Robots

Azka M. Burohman¹, Endra Joelianto^{1,2} and Augie Widyotriatmo¹

¹Instrumentation and Control Research Group, Faculty of Industrial Technology,
Institut Teknologi Bandung, Jl. Ganesha 10, Bandung 40132, Indonesia;

²National Center for Sustainable Transportation Technology, CRCS Building 2nd Floor,
Institut Teknologi Bandung, Jl. Ganesha 10, Bandung 40132, Indonesia;

Email : azka.mujiburohman@gmail.com, ejoel@tf.itb.ac.id (Corresponding author),
augie@tf.itb.ac.id

ABSTRACT

This paper presents a control design of multi-agent robot dynamic systems that drives multiple robots to move in a polygon formation while also avoiding collision with each other and possible obstacles. By placing the equilibrium of the system in a polygon formation configuration, the system succeeds to converge the robots' individual configuration at surrounding of the center point of the polygon formation. To obtain a collective goal objective, a state of the center point as a target point is defined in which its dynamic is stable and converges to the goal point. By using a smooth repulsive potential function, the robots are guaranteed to be safe from collisions with other robots in the formation and with obstacles. When a robot is at far from obstacle edges, the multi-agent robots form a polygon formation. The proof of multi-agent robots forming a polygon formation is shown by using the Lyapunov method. Simulations are carried out to show that the multi-agent robots develop a polygon formation and avoids collisions with each other and a static obstacle. Another advantage of the proposed algorithm is when one robot cannot continue to follow the group formation, the multi-robot system is able to re-coordinate with the remaining number of agents.

Keywords: Polygon formation, stability analysis, collision avoidance, multi-agent robots.

Mathematics Subject Classification: 62J12, 62G99

Computing Classification System: I.4

1. INTRODUCTION

Cyber-physical systems and networked control systems, which are familiarly called multi-agent or multi-robot controls, have been receiving considerable interest by researchers. The application of this system can be found in vehicle technology, such as transporting objects, platooning vehicle for energy efficiency, etc. Safety is also an important issue in the control design. However, the main objective of multi-robot motion control is to acquire global behavior, i.e., achieving and maintaining formation, and then reaching the goal. Hence, a control design that assures collision-free with obstacles is added as a secondary, but also a mandatory requirement.

Based on the data communication, a centralized control of multi-robot should manage lots computational data, while a decentralized control is a more relaxing method, which may reduce data consumption (Tanner et al., 2003), (Rezaee and Abdollahi, 2014). The centralized control usually

operates navigation-based data, while an onboard sensor is commonly used in the decentralized control, which may perform faster communication. Based on the advantages of each method, i.e., the centralized and the decentralized controls, the two methods can be combined. The centralized control that utilizes navigational feedback governs formation. On the other hand, the benefit of using the decentralized control with short range sensors is faster response behavior of the multi-agent robot system.

Several control design methods to maintain formation and to avoid obstacles for a vehicle robot have been proposed in the literatures (Gazi and Passino, 2003), (Olfati-Saber, 2006), (Barnes et al., 2007), (Barnes et al., 2009). Numerous methods use potential field or barrier function methods in solving collision avoidance problems. One problem in formation control is when the collision avoidance action could be executed in a real-time situation. Most approaches implement collision avoidance in the lower level control by means of the potential field or barrier function method (Ogren et al., 2001), (Namerikawa and Yoshioka, 2007), (Widyotriatmo and Hong, 2011), (Burohman et al., 2016), (Widyotriatmo et al., 2017). In (Yasuaki & Yoshiki, 2004) the heuristic method for collision avoidance of multiple mobile robots is presented. Hierarchical motion planning and control is also a solution for collision avoidance in multiple mobile robots (Haidegger, et al., 2011), (Purcaru et al., 2013). The mobile robot formation control using potential-field-based methods can handle changing environment.

In this paper, the generation of trajectories is operated by a smooth potential field method as a high-level control. The high-level control consists of a smooth potential attractive-repulsive, which determines the interaction between agents. A smooth potential function repulsive defining the interaction between agent and static obstacle and a quadratic-based attractive control to goal. In the low level of the control, the trajectory tracking control is implemented to follow the generated and desired formation configuration.

Every vehicle or robot has its dynamic behavior and constraint. In the case of wheeled vehicle, the nonholonomic constraint typically cannot be ignored. Generated trajectory from several algorithms is non-smooth, which cannot be reached by nonholonomic vehicle related to heading angle constraint. In this paper, the dynamic of nonholonomic robot and trajectory tracking control proposed in (Oriolo et al., 2002), (Do, 2007) are considered, and every desired trajectory is generated in real-time in such a way that a formation is configured smoothly, evading any collision, and reaching the desired goal.

Recently, the control rigid formation is also of interest rather than just random flocking (de Marina et al., 2015), (de Marina et al., 2016). The formation does not follow the virtual preliminary determined position but it is formed by the interaction between robots. Smooth collision avoidance in the formation makes the problem more complex. In this paper, the formation is built by placing the equilibrium system in a circular vicinity. Hence, a polygon formation is achieved. This work operates formation control surrounding the target, as in (Pei et al., 2016). It requires a stronger attraction from the target. Different with (Pei et al., 2016), this work considers dynamic target. The advantage of operating this scheme is that, in the case when one or more member(s) is broken or cannot continue the traveling due to lack of energy sources, the formation can stand still within the number of remaining robots. In the same sense, if the formation is added by new members, the polygon formation achieved in the

one larger polygon. The high- and low-level controllers are implemented together with the formation control. It is assumed that the communication topology of the multi robots is fixed and established. The switching communication topologies for cooperative control can be found in (Wang, et al., 2017).

The remainder of this paper is organized as follows. In Section 2, the graph theory, bump function, and the multi-agent system problem are formed. Section 3 elucidates the proposed control design. Simulation results are discussed in Section 4. The conclusion is drawn in Section 5.

2. PRELIMINARY AND PROBLEM STATEMENT

2.1. Graph Theory

The graph theory is the most suitable approach in multi-agent systems. It is able to define the relationship between agents in a group. The network topology model can be written as a graph $G = (\mathcal{V}, \mathcal{E})$, which consists of a vertex set $\mathcal{V} = \{u_1, u_2, \dots, u_N\}$ and an edge set $\mathcal{E} = \{(i, j) \in \mathcal{V} \times \mathcal{V}\}$. If the set of edge (i, j) and (j, i) are not differentiated, the graph is called as undirectional graph; otherwise, it is called as directional graph. Let the neighbor set of vertex i be N_i . The number of member of N_i is denoted as $\deg(u_i)$. A unidirectional graph, provided in this research, with N vertex has an adjacency matrix of $A = A(G) \in \mathfrak{R}^{N \times N}$ with the element as follows:

$$a_{ij} = \begin{cases} 1 & \text{if } i \neq j \text{ and } (i, j) \in \mathcal{E} \\ 0 & \text{otherwise} \end{cases} \quad (0)$$

The element of a matrix of degree $D = D(G) \in \mathfrak{R}^{N \times N}$ is defined as:

$$d_{ij} = \begin{cases} \deg(u_i) & \text{if } i = j \\ 0 & \text{otherwise} \end{cases} \quad (0)$$

Then, the element of the Laplacian matrix $L = D - A$, $L(G) \in \mathfrak{R}^{N \times N}$ of a graph G is defined as:

$$l_{ij} = \begin{cases} \deg(u_i) & \text{if } i = j \\ -1 & \text{if } i \neq j \text{ and } (i, j) \in \mathcal{E} \\ 0 & \text{otherwise} \end{cases} \quad (0)$$

The properties of the Laplacian matrix are as follows:

- $L(G)$ is symmetric and positive semi-definite.
- In order to make the graph connected, at most one eigenvalue can be zero, i.e. $\lambda_1 = 0$ and $\lambda_i > 0$ for $i \in \{2, \dots, N\}$
- The second smallest eigenvalue indicates the connectivity of the graph. Moreover, $null(L) = span(\mathbf{1}^N)$, where $null(\cdot)$ denotes the null space and $\mathbf{1}^N = (1, \dots, 1)^T \in \mathfrak{R}^N$.

Related to velocity matching in this paper, L satisfies the sum of square as follows:

$$z^T L z = \frac{1}{2} \sum_{(i,j) \in \mathcal{E}} a_{ij} (z_j - z_i)^2, \quad z \in \mathfrak{R}^N \quad (0)$$

The global minimum value of (4) is acquired when $z_i = z_j$.

2.2. σ - norm and Bump Function

This work considers a smooth potential function. To obtain potential function in the derivative of norm vector, it is used norm-like function called as σ - norm , defined as:

$$\|z\|_{\sigma} = \frac{1}{\varepsilon} \left[\sqrt{1 + \varepsilon \|z\|} - 1 \right] \quad (0)$$

with $\varepsilon > 0$, and its gradient $\sigma_{\varepsilon}(z) = \nabla \|z\|_{\sigma}$ is defined as:

$$\sigma_{\varepsilon}(z) = \frac{z}{\sqrt{1 + \varepsilon \|z\|}} = \frac{z}{1 + \varepsilon \|z\|_{\sigma}} \quad (0)$$

Bump function $\rho_h(z)$ is defined to conduct smooth cut-off function which is defined as:

$$\rho_h(z) = \begin{cases} 1 & z \in [0, h) \\ \frac{1}{2} \left[1 + \cos \left(\pi \frac{(z-h)}{(1-h)} \right) \right] & z \in [h, 1] \\ 0 & \text{otherwise} \end{cases} \quad (0)$$

where $h > 0$ is a positive constant between 0 and 1.

2.3. Problem Statement of Flocking of Multi-agent Systems

Consider the second order dynamic system of every agent i in the multi-agent system, which is determined as follows:

$$\begin{aligned} \dot{q}_i &= p_i \\ \dot{p}_i &= u_i \end{aligned} \quad \text{where } q_i, p_i, u_i \in \mathbb{R}^2 \quad (0)$$

q_i denotes position variable, p_i denotes velocity, and u_i denotes control signal of the i -th agent.

In (Olfati-Saber, 2006), this system consists of three protocols, which are as follow:

$$u_i = u_i^{\alpha} + u_i^{\beta} + u_i^{\gamma} \quad (0)$$

The first term u_i^{α} is the flocking configuration protocol determining interaction between agents, the second term u_i^{β} is the obstacle avoidance protocol, and the last term u_i^{γ} is the group trajectory attraction protocol. This control signal acts to send a group of robots to configure a flocking behavior and to avoid collision with any static obstacles in the environment, as well as move to reach the target point. Vectors $q = (q_1, q_2, \dots, q_N)^T$, $p = (p_1, p_2, \dots, p_N)^T$, and $u = (u_1, u_2, \dots, u_N)^T$ denote the collective position vector, the velocity vector, and the input signal vector, respectively.

The objective of this paper is to solve the problem in designing the controller of multi-agent dynamic systems, which converge to the equilibrium point. The equilibrium point for every agent robot is set to be every joint of a polygon. Furthermore, a safety requirement is not to be ignored. This work applies an obstacle avoidance method to avoid the multi-agent robots colliding with the other robot(s) in the group or with the static obstacle(s).

2.4. The Trajectory Dynamics

Overall, group members are guided by a center point, which is also acting as a temporary target point. The dynamic of the trajectory of this center point is denoted in (10). In the polygon formation, the state (q_c, p_c) is as a couple position and a velocity vector of formation center. The dynamics are as follows:

$$\begin{aligned}\dot{q}_c &= p_c \\ \dot{p}_c &= -k_{g1}(q_c - q_g) - k_{g2}(p_c - p_g)\end{aligned}\quad (0)$$

where (q_g, p_g) denotes position and velocity of a goal point and $k_{g1}, k_{g2} > 0$ is the positive constant. The dynamic system (10) is exponentially stable and converges to the goal point state. The center point dynamic (10) has not considered any obstacles in the environment.

3. CONTROL DESIGN

3.1. Control Design of Polygon Formation

The equilibrium point of a dynamic system could be shifted to a desired point. The equilibrium point in this case is shifted to a formation configuration, as the following details. In this analysis of formation realization, the obstacle avoidance control signal has not been considered or the formation could be conducted as if the arena is free from any static obstacles. By not taking into account the obstacle avoidance control signal, the control signal becomes:

$$u_i = u_i^\alpha + u_i^\gamma \quad (0)$$

The first term of (11) is defined as:

$$u_i^\alpha = k_{f1} \sum_{j \in N_i} \phi_\alpha(\|q_i - q_j\|_\sigma) n_{ij} + k_{f2} \sum_{j \in N_i} a_{ij} (p_j - p_i) \quad (0)$$

where $\phi_\alpha(\cdot)$ is defined as:

$$\phi_\alpha(\|q_i - q_j\|_\sigma) = \rho_b \left(\frac{\|q_i - q_j\|_\sigma}{r_\alpha} \right) \frac{\|q_i - q_j\|_\sigma - d_\alpha}{\sqrt{1 + (\|q_i - q_j\|_\sigma - d_\alpha)^2}} \quad (0)$$

where $k_{f1}, k_{f2} > 0$ are arbitrary positive constants, and d_α denotes the desired distance between agents. If the actual distance between two agents is larger than d_α , they will attract each other, and if the actual distance is smaller than d_α , they will push each other. This protocol is a gradient-based control of a potential function. r_α denotes the relationship range cutoff of each robot sensing capability. $\rho_b(\cdot)$ denotes the bump function in (7). n_{ij} denotes the unit vector of interaction between agents.

The second term of the control signal in (11) is the goal attraction control. It is a gradient-based control of a quadratic potential function defined as:

$$u_i^\gamma = -k_{c1}(q_i - q_c) - k_{c2}(p_i - p_c) \quad (0)$$

where $k_{c1}, k_{c2} > 0$ are positive constants.

The aggregate Lyapunov function candidate, which is also called as the potential field function of this system, is defined as follows:

$$H(q, p) = k_{f1}V_\alpha(q) + k_{c1}V_\gamma(q) + \frac{1}{2} \sum_i \|p_i\|^2 \quad (0)$$

where $k_{f1}, k_{f2}, k_{c1}, k_{c2} > 0$ denote positive constants, and $V_\alpha(z)$ is defined as

$V_\alpha(z) = \sum_i \sum_{j \in N_i} \psi_\alpha(z)$ which denotes the potential function attractive repulsive, where $\psi_\alpha(z)$ is defined as:

$$\psi_\alpha(z) = \int_{d_\alpha}^z \phi_\alpha(s) ds = \sqrt{1 + (z - d_\alpha)^2} - 1 \quad (0)$$

The illustration of this function $\psi_\alpha(z)$ trend is observed in Figure 1(a) and its gradient is in Figure 1(b). The function has minimum global with σ -norm domain at $z = \|q_i - q_j\|_\sigma = d_\alpha$. The values of positive constants determine the gradient of the curve in Figure 1, i.e., how strong the curve increases or decreases. The values of positive constants also determine the maximum value of working force. The boundedness of this smooth working force makes this control signal more realistic compared with a function in the form $1/z$ or $\log(z)$.

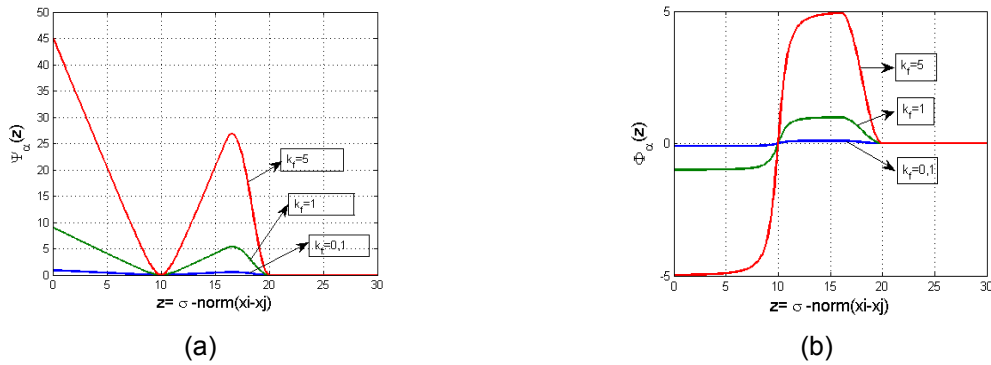


Figure 1. Potential function (a) and its gradient (b)

The second term of the aggregate potential function in (15) is the quadratic Lyapunov function, which is defined as follows:

$$V_\gamma(q) = \frac{1}{2} \sum_i \|q_i - q_c\|^2 \quad (0)$$

The third term of (15) denotes the kinetics energy of a particle with p_i as the velocity.

3.2. Collective Dynamic

In analyzing a system, it is necessary to define the system in one representation system. In a collective form, the dynamic of the overall group system is:

$$\begin{aligned}\dot{q} &= p \\ \dot{p} &= u = -k_{f1}\nabla V_a(q) - k_{f2}\hat{L}p + f^y(q, q_c)\end{aligned}\quad (0)$$

where $\nabla V_a(\cdot), q, \dot{q}, p, \dot{p}, u, f^y \in \mathfrak{R}^{2 \times N}$ and $\hat{L} \in \mathfrak{R}^{N \times N}$. Meanwhile, $f^y(q, q_c)$ is the attractive control to attract all agents to the center point, denoted as:

$$f^y(q, q_c, p, p_c) = -k_{c1}(q - \mathbf{1}_N \otimes q_c) - k_{c2}(p - \mathbf{1}_N \otimes p_c). \quad (0)$$

Vector $\mathbf{1}_N$ denotes as $\mathbf{1}_N = (1, 1, \dots, 1)^T \in \mathfrak{R}^N$ and notation \otimes defines the *Kronecker product*.

3.3. Stability Analysis of Formation Control

This section analyzes how the polygon or also well called as circle formation is built by the control design. Consider the Lyapunov function in (15), the time derivation along the solution of dynamic system (10) is determined in the following equation:

$$\dot{H}_2(q_{tr,i}) = -k_{c2}(p_{tr}^T \hat{L} p_{tr}) - 2k_{c2} \left(T(q_{tr}, p_{tr}) - \frac{n}{2}(\bar{p} \cdot p_c) \right) < 0, \quad (0)$$

where $T(q, p) = \frac{1}{2} \sum_i \|p_i\|^2$, \bar{p} denotes the average of all agent velocity.

The second term of inequality (20) is assumed to be positive definite. This assumption means that the absolute velocity for every agent is larger than the multiply of average and the velocity of the goal point (Olfati-Saber, 2006). Furthermore, if it is assumed that the polygon formation is in regard to the target point q_c , the value of p_c is assumed zero. Hence, the energy function $H(q)$ is a decreasing function along the solution of the dynamic of multi-agent system.

Assumption 1: There are chosen positive constants $k_{f1}, k_{c1}, k_{f2}, k_{c2}$ such that the equilibrium of (18) is not convergent to the condition $q_i = q_c$.

Assumption 2: There is a space where it is collision-free or $u_i^p = 0$.

Theorem 3.1. Suppose that assumptions 1 and 2 are hold, the multi-agent system (18) operates control signal (12), based on the fact that the Lyapunov function (15) decreases, the equilibrium system is asymptotically stable in regard to the target point q_c , and at the same time, the position state of each agent converge to polygon configuration if $N \geq 4$.

Proof:

Based on the Lyapunov stability theorem and LaSalle's invariant principle, the equilibrium system is asymptotically stable and converges to the largest invariant set of the dynamic system, i.e., $\{q \mid \dot{H}_2(q) = 0\}$. The velocity matching is achieved from the first term by property of graph Laplacian equality to sum of square. The second term determines the velocity of each agent match to the velocity of trajectory dynamic agent q_c . Moreover, the system converges to unique equilibrium

q^* , which, in the other word, converges to the extrema of $k_{f1}V_\alpha + k_{c1}V_\gamma$, i.e. $-k_{f1}\nabla V_\alpha(q) + f^\gamma(q, q_c) = 0$. Configuration of formation is formed when the system is in the equilibrium point, as the following equation:

$$k_{f1} \sum_{j \in N_i} \varphi_\alpha(q_i - q_j) n_{ij} = k_{c1}(q_i - q_c). \quad (20)$$

Equation (21) geometrically indicates that the position of each agent is balanced surrounding the target point q_c . According to Theorem 3.2 in (Pei et al., 2016), the sufficient condition to the dynamic target pursuit is given by

$$d_c \cos \frac{\pi}{N} \geq \frac{1}{2} d \quad (22)$$

where d_c denotes the distance of q_i to q_c , and d denotes the distance between two agents, i.e., q_i to q_j . The cancelation of repulsive and attractive forces among agents result in the value of d_c close to d . Then, the inequality (22) states that the polygon formation is realized if the number of agents is more than or equals to 4. \square

3.3. The Case of Obstacle Avoidance

In this paper, we consider the smooth potential field method to obtain the obstacle avoidance scheme. We use the smooth potential because its implementation is realistic. There is an additional term in control scheme, which is:

$$u_i^\beta = -\nabla F_i^\beta(q_i, p_{obs}). \quad (23)$$

The function $F_i^\beta(\cdot)$ in (23) is defined as:

$$F_i^\beta(q_i, q_{obs}) = \sum_k \psi_\beta(\|q_i - q_{obs,k}\|) \quad (24)$$

where $q_{obs,k}$ could be a function of state q_i , according to Lemma 3 in (Olfati-Saber, 2006), the notation $q_{obs,k}$ can be written as $\hat{q}_{i,k}$. The function $\psi_\beta(\cdot)$ satisfies the following characteristics:

- 1) $\psi_\beta(\|q_i - q_{obs}\|)$ increasing at a maximum certain value when $\|q_i - q_{obs}\| \rightarrow 0$;
- 2) $\psi_\beta(\|q_i - q_{obs}\|) \rightarrow 0$ as $\|q_i - q_{obs}\| \rightarrow d_\beta$;
- 3) $\psi_\beta(\|q_i - q_{obs}\|) = 0$ if $\|q_i - q_{obs}\| > d_\beta$.

One example of functions that satisfies the requirement is as follows:

$$\psi_\beta(z) = \int_{d_\beta}^z \varphi_\beta(s) ds = \rho_h(z/d_\beta) \left(\sqrt{1 + (z - d_\beta)^2} - (z - d_\beta) \right) \quad (25)$$

The control action based on the smooth repulsive potential function in (25) is determined as:

$$u_i^\beta = k_{o1} \sum_{k \in N_i^\beta} \varphi_\beta \left(\|\hat{q}_{i,k} - q_i\|_{o1} \right) n_{ik} + k_{o2} \sum_{k \in N_i^\beta} b_{i,k} (\hat{p}_{i,k} - p_i) \quad (26)$$

where $\varphi_\beta(\cdot)$ is defined as:

$$\varphi_\beta(z) = \rho_h(z/r_\beta) \left(\frac{z - d_\beta}{\sqrt{1 + (z - d_\beta)^2}} - 1 \right) \quad (27)$$

Figure 2 shows the repulsive potential function and its gradient.

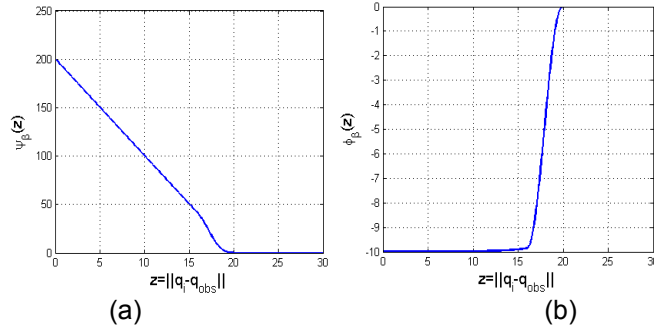


Figure 2. (a) Repulsive potential function and (b) the gradient of repulsive potential function

Theorem 3.2. Suppose that there are chosen positive constants $k_{f1}, k_{f2}, k_{c1}, k_{c2}, k_{o1}, k_{o2} > 0$ such that the $c^* > H(q(0), p(0))$, where $c^* = \psi_\beta(0)$, or where an agent collides with static obstacle and $H(q(0), p(0))$ is the initial condition of the system. Then, by operating control signal (9) with (12), (14), and (26), the system satisfies the following properties:

- 1) Every robot in formation is driven to the vicinity of obstacle's influence-free;
- 2) Every robot is guaranteed not to collide with a static obstacle;
- 3) The polygon formation is destructed when obstacles appear, and restore in when it is obstacles-free.

Proof:

The total energy function of the multi-agent robots with an obstacle in the environment is determined as:

$$H(q, p) = k_f V_a(q) + k_o V_\beta(q, \hat{q}) + k_{c1} V_y(q) + \frac{1}{2} \sum_i \|p_i\|^2. \quad (28)$$

According to the Theorem 6 in (Olfati-Saber, 2006), the energy of the system monotonically decreases. Hence, due to the energy increases as the robots going near the obstacle boundary, the trajectory of the robots is driven until converge to the origin, i.e. the vicinity of obstacle influence, the first part is proven.

The second part of this theorem is proved by contradiction. Suppose that if an agent is collided at time t , it has $c^* > H(q(0), p(0))$. If an agent collides, then

$$k_f V_\alpha(q(t)) + k_o V_\beta(q(t), \hat{q}(t)) + k_{c1} V_\gamma(q(t)) + \frac{1}{2} \sum_i \|p_i(t)\|^2 > k_o V_\beta(q(t), \hat{q}(t)) \quad (29)$$

However, we have $H(q, p)$ as a decreasing energy function, hence $H(q(0), p(0)) > H(q(t), p(t)) > c^*$ which contradicts the beginning statement.

The third part of the theorem is proved by the fact that the largest invariant set, which becomes the sink of the convergence is not in (20), then the polygon formation is destructed. After it is free from obstacle effect, the second term of energy function is cancelled, i.e., $V_\beta = 0$, then system is in the free obstacle condition and the equilibrium related to the center point is re-coordinated in the circular vicinity. \square

3. SIMULATION RESULTS

3.1. Simulation Setting

To verify that our algorithm works for some multi-agent robots, we operate this algorithm in a group of nonholonomic robots. The heading constraint of nonholonomic robots is solved by trajectory tracking algorithm via dynamic feedback linearization in (Oriolo et al., 2002). In the simulation, we consider four scenarios: hexagonal formation in free space, enlarge the size of the polygon formation with 15 members, hexagon formation with static obstacle in space, and polygon formation reforming when one robot cannot continue traveling.

The constant parameters implemented in this simulation are as follow: $\varepsilon = 2$, $d_\alpha = 20$, $r_\alpha = 25$, $k_{f1} = 6.1317$, $k_{f2} = 0.5269$, $k_{c1} = 0.2302$, $k_{c2} = 4,0155$. Meanwhile, the constant gain parameters for trajectory dynamic are chosen as: $k_{g1} = 0.229$, $k_{g2} = 3.966$.

3.2. Polygon Formation in Free-obstacle Environment

In the first simulation, six robots move in hexagon formation. The initial condition is randomly placed near point $q_0 = (x_0, y_0) = (-90, -90)$ with the initial velocity $p = (v_x, v_y) = (0, 0)$ for every robot i . The group in formation stops when they surrounding goal point at $(q_g, p_g) = (80, 80)$. We can change this goal point anywhere. The first scenario of the simulation result is depicted in Figure 3. In 30 seconds, the robot team forms the hexagonal shape. The quickness of the group to make a polygon formation depends on the value of k_{f1} and k_{f2} .

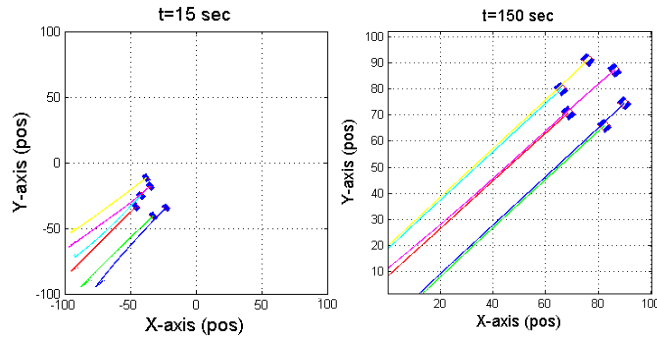


Figure 3. Simulation of hexagon formation in an obstacle-free environment

Furthermore, the simulation provides a larger number of groups with 15 members in Figure 4 to show that the algorithm works for any number of robots. The size of the formation, i.e., the number of group members, is related to the constant gain election. We have to choose the constant gain properly to obtain the best performance.

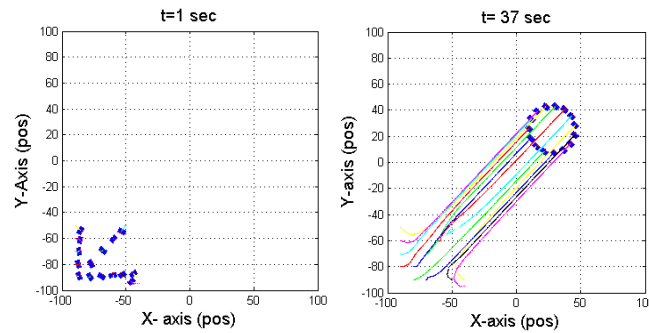


Figure 4. Simulation of polygon formation of 15 robots moving in free-obstacle area

Another advantage of using this stabilization formation algorithm is when one member of the group lack of energy, hence it cannot continue to travel with other robots. The simulation results in Figure 5 show that the pentagon formation is immediately reformed automatically from the hexagon formation, which is missing their formation member.

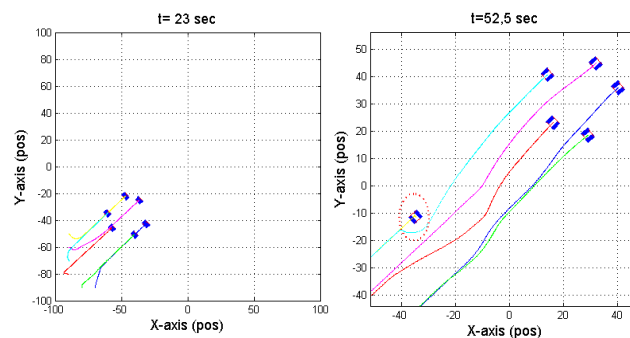


Figure 5. Simulation of case when one agent cannot continue the traveling

3.3. Robot Formation with a Static Obstacle in the Environment

For the case of robot formation with a static obstacle in the environment, the simulation of the hexagon formation shows the destructed formation due to the existence of a static obstacle in the way (Figure 6). After passing through the obstacle, the group of robots reforms the polygon formation. We place the static circular obstacle with the center at $(0,10)$. The parameters for repulsive force are $d_{\beta} = 20$, $k_{o1} = 5$, and $k_{o2} = 1.5$.

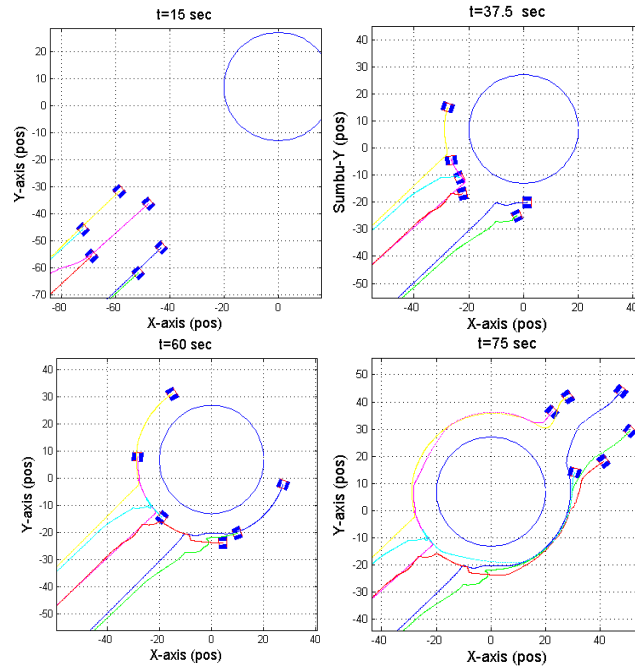


Figure 6. Simulation of 6 robots with a static obstacle.

5. CONCLUSION

The paper proposed a controller to obtain a polygon formation for second-order multi-agent robots. The formation of the multi-agent robots was achieved by placing the equilibrium to the force balance of polygon geometry. The simulation scenarios of 6 robots making a hexagon formation, 15 robots making a polygon formation, 6 robots with one robot failure making a pentagon formation, and 6 robots with a static obstacle showed that the proposed algorithm can work for any number of robots and for a case where a static obstacle occurred in the environment. Furthermore, this work considered the obstacle avoidance such that the formation of robot avoiding collision with a static obstacle in the environment.

ACKNOWLEDGMENT

This work was supported by the Ministry of Research, Technology, and Higher Education Republic of Indonesia and Institut Teknologi Bandung. This research was partially funded by USAID through the SHERA program – Centre for Collaborative (CCR) National Center for Sustainable Transportation Technology (NCSTT) – ITB with Contract No. IIE0000078-ITB-1.

REFERENCES

- Barnes, L., Fields, M., Valavanis, K., 2007, Unmanned ground vehicle swarm formation control using potential fields. In *2007 Mediterranean Conference on Control & Automation MED'07*, 1-8. IEEE.
- Barnes, L.E., Fields, M.A., Valavanis, K.P., 2009, Swarm formation control utilizing elliptical surfaces and limiting functions. *IEEE Transactions on Systems, Man, and Cybernetics, Part B (Cybernetics)* **39**, 6, 1434-1445.
- Burohman, A.M., Widyotriatmo, A., Joelianto, E., 2016, Flocking for nonholonomic robots with obstacle avoidance. In *2016 International Electronics Symposium (IES)*, 345-350. IEEE.
- de Marina, H.G., Cao, M., Jayawardhana, B., 2015, Controlling rigid formations of mobile agents under inconsistent measurements. *IEEE Transactions on Robotics* **31**, 1, 31-39.
- de Marina, H.G., Jayawardhana, B., Cao, M., 2016, Distributed scaling control of rigid formations. In *2016 IEEE 55th Conference on Decision and Control (CDC)*, 5140-5145. IEEE.
- de Marina, H.G., Jayawardhana, B., Cao, M., 2016, Distributed rotational and translational maneuvering of rigid formations and their applications. *IEEE Transactions on Robotics* **32**, 3, 684-697.
- Do, K.D., 2007, Formation tracking control of unicycle-type mobile robots. In *2007 IEEE International Conference on Robotics and Automation*, 2391-2396. IEEE.
- Gazi, V., Passino, K.M., 2003, Stability analysis of swarms. *IEEE Transactions on Automatic Control* **48**, 4, 692-697.
- Haidegger, T., Kovacs, L., Preitl, S., Precup, R.-E., Benyo, B. Benyo, Z. 2011, Controller design solutions for long distance telesurgical applications. *International Journal of Artificial Intelligence* **6**, S11, 48-71.
- Namerikawa, T., Yoshioka, C., 2007, Formation Control of Nonholonomic Multi-Vehicle Systems via Virtual Structure. In *Proc. of Fourth International Conference on Computational Intelligence Robotics and Autonomous Systems*, 202-207.
- Ogren, P., Egerstedt, M., Hu, X., 2001, A control Lyapunov function approach to multi-agent coordination. In *Proceedings of 40th IEEE Conference on Decision and Control*, **2**, 1150-1155. IEEE.
- Oriolo, G., De Luca, A., Vendittelli, M., 2002, WMR control via dynamic feedback linearization: design, implementation, and experimental validation. *IEEE Transactions on Control Systems Technology* **10**, 6, 835-852.
- Olfati-Saber, R., 2006, Flocking for multi-agent dynamic systems: Algorithms and theory. *IEEE Transactions on Automatic Control* **51**, 3, 401-420.
- Pei, H., Chen, S., Lai, Q., 2016, Multi-target consensus circle pursuit for multi-agent systems via a distributed multi-flocking method. *International Journal of Systems Science* **47**, 16, 3741-3748.
- Pucaru, C., Precup, R.-E., Ierican, D., Fedorovici, L.-O., David, R.-C., Dragan, F. 2013, Optimal robot path planning using gravitational search algorithm, *International Journal of Artificial Intelligence* **10**, S13, 1-20.
- Rezaee, H., Abdollahi, F., 2014, A decentralized cooperative control scheme with obstacle avoidance for a team of mobile robots. *IEEE Transactions on Industrial Electronics* **61**, 1, 347-354.
- Tanner, H.G., Jadbabaie, A., Pappas, G.J., 2003, Stable flocking of mobile agents, Part I: Fixed topology. In *Decision and Control, 2003. Proceedings. 42nd IEEE Conference on*, **2**, 2010-2015. IEEE.
- Tanner, H.G., Jadbabaie, A., Pappas, G.J., 2003, Stable flocking of mobile agents, Part II: Dynamic topology. In *Proceedings of 42nd IEEE Conference on Decision and Control*, **2**, 2016-2021.

Wang, B., Wang, J., Zhang, L., Zhang, B., Li, X., 2016, Cooperative control of heterogeneous uncertain dynamical networks: An adaptive explicit synchronization framework. *IEEE Transactions on Cybernetics* **47**, 6, 1484-1495.

Widyotriatmo, A., Hong, K.S., 2011, Navigation function-based control of multiple wheeled vehicles. *IEEE Transactions on Industrial Electronics* **58**, 5, 1896-1906.

Widyotriatmo, A., Joelianto, E., Prasdianto, A., Bahtiar, H., Nazaruddin, Y.Y., 2017, Implementation of leader-follower formation control of a team of nonholonomic mobile robots. *Int. J. Comput. Commun. Control* **12**, 6, 871-885.

Yasuaki, A., Yoshiki, M., 2004, Real-time cooperative collision avoidance method of multiple mobile robots. *Proceedings of 5th IFAC/EURON Symposium on Intelligent Autonomous Vehicles*, Instituto Superior Técnico, Lisboa, Portugal, July 5-7, 2004, 30-35.